



# In situ observations of a reduction in effective crystal diameter in cirrus clouds near flight corridors

A. Kristensson, J.-F Gayet, J. Ström, F. Auriol

## ► To cite this version:

A. Kristensson, J.-F Gayet, J. Ström, F. Auriol. In situ observations of a reduction in effective crystal diameter in cirrus clouds near flight corridors. *Geophysical Research Letters*, 2000, 27 (5), pp.681-684. 10.1029/1999GL010934 . hal-01895776

HAL Id: hal-01895776

<https://uca.hal.science/hal-01895776>

Submitted on 15 Oct 2018

**HAL** is a multi-disciplinary open access archive for the deposit and dissemination of scientific research documents, whether they are published or not. The documents may come from teaching and research institutions in France or abroad, or from public or private research centers.

L'archive ouverte pluridisciplinaire **HAL**, est destinée au dépôt et à la diffusion de documents scientifiques de niveau recherche, publiés ou non, émanant des établissements d'enseignement et de recherche français ou étrangers, des laboratoires publics ou privés.

# In situ observations of a reduction in effective crystal diameter in cirrus clouds near flight corridors

A. Kristensson<sup>1</sup>, J.-F. Gayet<sup>2</sup>, J. Ström<sup>1</sup> and F. Auriol<sup>2</sup>

**Abstract.** Measurements of the crystal size distribution performed over Southern Germany show that the effective diameter decrease 10–30% in cirrus clouds perturbed by aircraft. The reduction is more pronounced at higher cloud water content and is not observed at temperatures warmer than -30°C.

## Introduction

Concurrent with the increase in use of aviation fuel, observations show an increase in the frequency of occurrence and area coverage of cirrus clouds in the main flight routes [Boucher, 1999; Mannstein *et al.*, 1998]. The radiative forcing due to increased cloudiness is believed to be small on a global scale, but could approach 1 W m<sup>-2</sup> regionally [Fahey and Schumann, 1999; Boucher, 1999]. Aircraft exhaust may also alter the optical properties of natural cirrus clouds, but despite growing insight in the early development of the plume in the aircraft wake [e.g. Schumann *et al.*, 1996; Kärcher *et al.*, 1998], the role of aircraft exhaust in modifying cirrus is still an open question.

Ström and Ohlsson [1998], hereafter S&O addressed this problem and observed that the crystal number density ( $N_c$ ) is enhanced about a factor two in cirrus clouds where the soot content exceeded 0.01 µg m<sup>-3</sup> compared to cirrus with less soot. An elevated soot content was assumed to originate from aircraft exhaust. If the cloud water content (CWC) is not affected by aircraft exhaust, a two-fold increase in  $N_c$  would translate into a reduction of the mean crystal size by about 20%. A preliminary study by Wyser and Ström [1998] suggests that such reduction in crystal size can induce a radiative forcing equal in magnitude to that caused by the contrail cloudiness. A similar conclusion was reached by Meerkötter *et al.* [1999].

In this study the data set used by S&O has been extended to include measurements of the cirrus crystal size distribution,  $N_c(d)$ , which makes it possible to explicitly compare the crystal size in perturbed and unperturbed cirrus, hereafter  $Ci^*$  and  $Ci$  respectively.

## Experimental

During the AEROCONTRAIL project in October 1996 an aerosol and cloud microphysical payload was mounted on the research aircraft Falcon, operated by Deutsches Zentrum für

Luft- und Raumfahrt. The objective of the experiment was to study the evolution of young aircraft plumes, from contrails into a cirrus-like stage. At times when there was no suitable aircraft to chase, the flights were devoted to characterization of cirrus clouds. The flights were conducted in an air space over southern Germany that is very busy in terms of air traffic.

A PMS Forward Scattering Spectrometer Probe 100 (FSSP-100) [Dye and Baumgardner, 1984] and a PMS 2DC-probe [Knollenberg, 1969] were used to measure the crystal size distribution. The FSSP measures the number density in 15 size classes between 2-32, 2-47 and 5-95 µm in diameter depending on range setting, which most of the time was 2-47 µm. Crystals passing the probe area are illuminated by a laser beam and the measured scattered light is inverted to particle size using Mie theory [Gayet *et al.*, 1996a]. The 2DC probe classifies particles in 30 size classes between 12.5-762.5 µm in diameter. A laser illuminates an array of pixels, which will register the shadow caused by a crystal crossing the laser beam.

To differentiate between  $Ci^*$  and  $Ci$ , the amount of absorbing material in the crystals, equivalent to the soot content was determined. The crystals were extracted from the ambient air using a Counterflow Virtual Impactor probe (CVI) [Noone *et al.*, 1988; Ström *et al.*, 1997] with a lower and upper cut-off size 4.5 and 60 µm in aerodynamic diameter, respectively. The crystals are evaporated inside the CVI by a warm and dry carrier air stream and the non-volatile residual particles that are left behind are counted using a condensation particle counter (CPC), TSI-3760 (TSI, Inc., St Paul, MN). The concentration of absorbing material contained

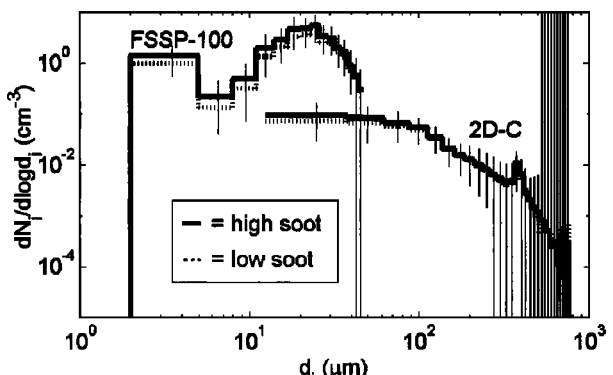


**Figure 1.** The average crystal size distribution from October 15<sup>th</sup>, 1996 for crystals with high and low soot content. The crystal diameter is denoted by  $d$  and the CWC ranges from 50 to 700 mg·m<sup>-3</sup>. Vertical bars cover crystal number densities between the 10 and 90 percentile for  $Ci^*$ . With a t-test the difference in  $N_c$  between  $Ci^*$  and  $Ci$  is shown to be significant for all bins in the FSSP except the last 2 and in the 2DC the high soot density is significantly higher for the 4 first bins.

<sup>1</sup> Institute of Applied Environmental Research, Air Pollution Laboratory, ITML, Stockholm University, Stockholm, Sweden

<sup>2</sup> Laboratoire de Météorologie Physique, URA CNRS 267, Université Blaise Pascal, Clermont-Ferrand, France

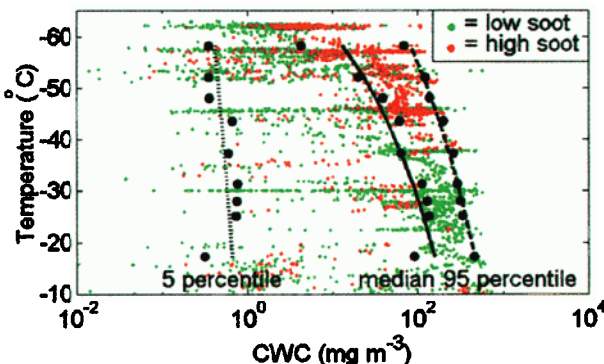


**Figure 2.** Scatter plot of  $T$  versus CWC for both high and low soot data. Black dots correspond to percentiles of CWC in 15°C temperature windows which are shifted at 5°C intervals. Lines are exponential fits to black data points.

in the residue particles was measured by a Particle Soot Absorption Photometer (PSAP, Radiance Res., Seattle, WA). The PSAP measures the change in optical transmission caused by residual particles depositing on a filter, and the light source used in the PSAP is 550 nm. The equivalent soot content was calculated using a specific absorption coefficient  $10 \text{ m}^2 \text{ g}^{-1}$ . Sample air in the CVI is enriched a factor 100 relative to ambient conditions, which results in an effective detection limit of the PSAP instrument of  $0.01 \mu\text{g m}^{-3}$  at 5 seconds integration time. Finally, a CPC with a lower cut-off at  $0.007 \mu\text{m}$  was connected to a submicrometer inlet facing the opposite flight direction to measure the ambient aerosol number density [Schröder and Ström, 1996].

### Data reduction

As in the study by S&O, the goal is to investigate the effect on cirrus by aged exhaust and to exclude the contribution from fresh contrails. For this reason the aerosol number density and  $N_c$  are limited to values below  $1500 \text{ cm}^{-3}$  and  $30 \text{ cm}^{-3}$  respectively. During the measurements, the FSSP probe was mounted under one of the wings and the CVI on top of the fuselage and thin or patchy cirrus was sometimes only observed by one of the two instruments. To exclude these situations, data was further reduced through the criteria, that  $N_c$  measured by the two probes must exceed  $0.05 \text{ cm}^{-3}$  simultaneously. The resulting data from the two instruments is well correlated, although the  $N_c$  of the CVI is on average 50% larger than the FSSP. The exact reason for this is

unknown. However, this is not critical to the analysis in this study, since  $N_c$  measured by the CVI is not part of the determination of the crystal size characteristics.

The 4768 remaining data points are grouped according to the amount of absorbing material contained in the crystals. If the equivalent soot concentration observed by the CVI is below  $0.01 \mu\text{g m}^{-3}$  in the cloud, the data points belong to the category  $C_i$ . Otherwise, the data belong to the category  $C_i^*$ , which includes 41% of the cases.

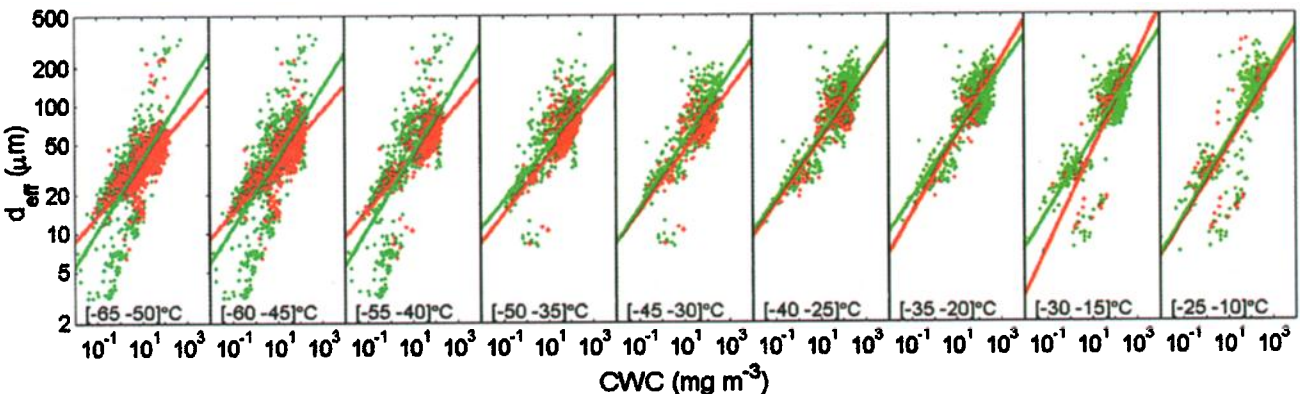
### Results

Figure 1 presents an example of an average crystal size distribution observed by the FSSP and 2DC probe on the flight 15 October for  $C_i^*$  and  $C_i$ . Most crystals in the cirrus are in the range of the FSSP between 20–30  $\mu\text{m}$  in diameter. The instrument shows enhanced  $N_c$  in the perturbed case by about a factor 1.5, whereas the two curves for the 2DC probe show smaller difference.

Note that the measurements of  $N_c(d)$  by the PMS probes and the measurements of absorbing material in crystals by the CVI probe are completely independent. There is a concern that the assumption of one residual particle equaling one crystal, used to derive  $N_c$  from CVI measurements, is not always valid and that a single crystal can give rise to multiple residuals. This problem is alleged to occur as a result of crystal break up or by insoluble particles sticking on the surface of the crystals. Since this potential sampling problem has no influence on  $N_c(d)$  it does not enter the analysis.

However, simply comparing average  $N_c(d)$  between the  $C_i^*$  and  $C_i$  categories may be misleading, because of the limited data set and the large natural variability in cirrus. The large natural variability in the microphysical properties can be seen from the large range in the 10- and 90-percentiles for each size class in Figure 1. Differences in ambient temperature ( $T_a$ ) and CWC may mask the effect by aircraft exhaust on the mean crystal size. Therefore, we have made an attempt to reduce the influence from these parameters, by analyzing clouds in separate temperature regimes and specific CWCs.

The CWC was calculated from the  $N_c(d)$  using relations given by Gayet *et al.*, [1996a] for the FSSP probe and Gayet *et al.*, [1996b] with particle recognition specified by Darlison and Brown, [1988] for the 2DC probe. The contribution from the FSSP and 2DC probe was added together despite the fact that there is a region of overlap (c.f. Figure 1). This is not a large error, since the contribution from the 2DC probe is much less than the contribution from the FSSP probe in this region,



**Figure 3.** Scatter plot of  $d_{\text{eff}}$  versus CWC in each temperature interval. Lines are linear fits to the  $C_i^*$  and  $C_i$  cases.

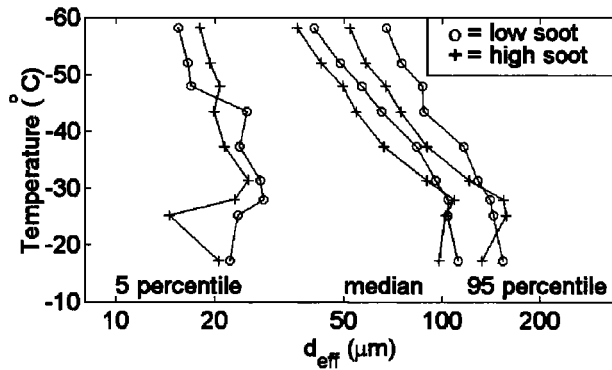


**Figure 4.** T versus  $d_{\text{eff}}$ . The three relations of  $d_{\text{eff}}$  are derived from the fitted CWC percentiles in Figure 2 using the relations in Figure 3.

which is probably caused by the irregular shape of crystals [Gayet *et al.*, 1996a]. Moreover, because the data is treated the same way for  $C_i^*$  and  $C_i$  any systematic error should be canceled when the two cases are compared. For the same reason only crystals smaller than 45  $\mu\text{m}$  diameter were used in the FSSP size distribution when the range setting was 5–95  $\mu\text{m}$ , which comprises 11% of the data points.

A scatter plot between the derived CWC and  $T_a$  is presented in Figure 2. As expected, the CWC range over several orders of magnitude for a given  $T_a$  and the maximum CWC decrease with decreasing  $T_a$ . Values are mostly in the range given in the literature for cirrus [Dowling and Radke, 1990]. Notice that the CWC is calculated for cirrus, although liquid drops may be present at  $T_a$  above the homogeneous freezing temperature ca. -40°C.

Data points for  $C_i^*$  and  $C_i$  in Figure 2 are marked with red and green symbols, respectively. Ideally, we would like to compare these two cases for a given  $T_a$  and CWC. However, this is not feasible and we need to come up with a way to bin the data. We proceed by calculating the 5-, 50-, and 95-percentile for CWC as a function of  $T_a$ , using data points for both  $C_i^*$  and  $C_i$ . To avoid that our choice of bin limits affects our results we use a 15°C window that is shifted in steps of 5°. This effectively generates a smoothing of the data. Different combinations of interval and step were tried, but this combination gave the best balance between resolution and scatter. The resulting mean percentiles in CWC for each 15-degree interval are plotted as filled circles in Figure 2 and a simple exponential curve is fitted to the data points.

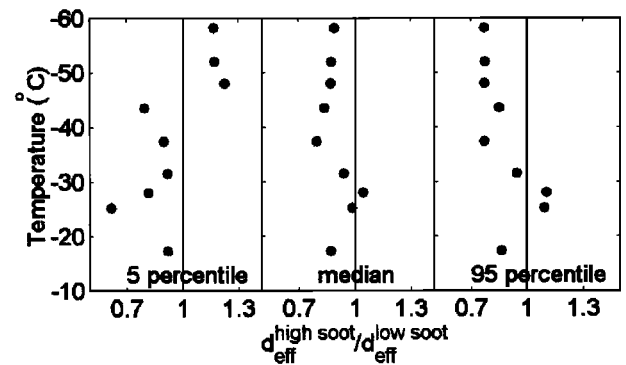


**Figure 5.** T versus ratio of high to low soot  $d_{\text{eff}}$ . The ratio is calculated using data presented in Figure 4.

In Figure 3 we present a scatter plot between the effective diameter ( $d_{\text{eff}}$ ) and CWC for each temperature interval.  $d_{\text{eff}}$  is defined as the third moment of  $N_C(d)$  divided by the second moment. A curve is fitted to each of the two cirrus types as shown in Figure 3. Using these relations we can compare  $d_{\text{eff}}$  for  $C_i^*$  and  $C_i$  as a function of  $T_a$  and CWC percentile, which is presented in Figure 4. For low values of CWC,  $d_{\text{eff}}$  decreases slowly with decreasing  $T_a$ . For median and high values of CWC the decrease in  $d_{\text{eff}}$  with decreasing  $T_a$  is more pronounced. However, the most interesting observation is the systematic difference in  $d_{\text{eff}}$  between  $C_i^*$  and  $C_i$  at average temperatures below -30°C. Table 1 gives absolute values of results presented in Figures 2 and 4. The errors associated with derived parameters such as  $d_{\text{eff}}$  and CWC may exceed 30% [Larsen *et al.*, 1998].

It is the fractional change in  $d_{\text{eff}}$  that more correctly reflects a change in  $N_C$ , that was depicted in Figure 1. The ratio between the perturbed and unperturbed  $d_{\text{eff}}$  is consequently presented in Figure 5. As seen in the figure,  $d_{\text{eff}}$  in  $C_i^*$  is systematically 10 to 30 percent smaller at  $T_a$  below -30°C for median and 95 percentile CWC. This is the expected reduction in size if  $N_C$  is enhanced a factor 1.5–3 while keeping the CWC unchanged. The observed ratio between the crystal number densities ranges from 1.4 to 2.7 in the five coldest intervals as shown in Table 1. But in the four warmest intervals the ratio is much less, 0.1–0.6 and no clear trend is observed for  $d_{\text{eff}}$ . However,  $N_C$  is averaged over the bulk of the CWC in each temperature interval. This approach was intentionally avoided in the foregoing analysis, which led to

**Table 1.** Cirrus cloud microphysical properties versus 9 temperature interval with widths 15°C and a 5°C step.  $N_7$  is the number density of aerosols larger than 7 nm and  $N_C^*/N_C$  the ratio of median crystal number density between high and low soot content.

Temp. interval (°C)	Mean temp. (°C)	CWC (mg m <sup>-3</sup> )			$d_{\text{eff}} (\mu\text{m})$ (high/low soot content)						No. of data points	% data points perturbed	Median $N_7$ (cm <sup>-3</sup> )	$N_C^*/N_C$					
		5% tile	Median	95% tile	5%tile		Median		95%tile										
					high	low	high	low	high	low									
[-65–50]	-58.2	0.412	13.1	82.8	18.0	15.4	35.9	40.3	51.9	67.3	2153	40	342	2.3					
[-60–45]	-52.0	0.445	23.6	118	19.3	16.5	42.4	48.5	58.3	75.2	1906	42	517	2.7					
[-55–40]	-48.0	0.468	32.4	145	20.6	16.8	49.3	56.6	67.1	86.9	1331	39	655	2.2					
[-50–35]	-43.5	0.494	44.3	179	19.9	25.0	54.5	65.3	74.6	87.9	1131	33	821	2.1					
[-45–30]	-37.4	0.531	63.8	232	21.4	23.9	66.5	83.5	90.2	117	639	27	836	1.4					
[-40–25]	-31.4	0.568	87.0	291	25.4	27.6	89.9	95.7	122	129	988	13	1011	0.6					
[-35–20]	-28.0	0.590	102	329	23.1	28.3	109	105	155	141	869	9	1183	0.5					
[-30–15]	-25.2	0.609	116	361	14.5	23.5	103	104	157	144	838	8	1144	0.6					
[-25–10]	-17.3	0.662	158	462	20.5	22.3	98.0	113	133	154	483	14	617	0.1					

the results presented for  $d_{\text{eff}}$ . The values of the crystal density ratios should therefore be regarded with care.

## Discussion and conclusion

Although, we do not understand the mechanism that cause the enhanced  $N_c$ , heterogeneous ice nuclei present in sufficient numbers could explain the observations as suggested by *Jensen and Toon* [1997]. Since the shift in the ratio of the crystal size occurs around  $-30^\circ\text{C}$  as shown in Figure 5, it is tempting to interpret this as if the responsible mechanism depends on the cloud actually glaciating.

The presence of super-cooled or liquid clouds is rare at  $T_a$  below  $-30^\circ\text{C}$ , whereas the chance is about 50% to find a liquid cloud at  $-15^\circ\text{C}$  [*Rogers and Yau*, 1989]. At the colder temperatures details in the freezing mechanism determines the number of crystals formed, but at warmer temperatures heterogeneous nuclei can be the difference between the cloud actually freezing or remaining liquid.

An ice crystal surrounded by water drops will grow quickly on the expense of the drops. Hence, if freezing is initiated by particles from aircraft exhaust, the contaminated data points could be associated with fewer but larger particles at warmer temperatures. Heterogeneous freezing is known to be temperature dependent and some ice nuclei do not become active until  $T_a$  decreases below a certain threshold value. If this  $T_a$  is as low as  $-30^\circ\text{C}$  for aircraft exhaust particles, an effect on crystal size at higher  $T_a$  would not be present.

On the other hand, this apparent shift around  $-30^\circ\text{C}$  may be purely coincidental due to the small fraction of data points classified as  $\text{Ci}^*$  in the warmer intervals. As shown by *S&O* this fraction closely follows the vertical distribution of the use of aviation fuel. Since temperatures at the preferred flight levels usually are colder than  $-30^\circ\text{C}$ , the statistics suffer from the lack of data from  $\text{Ci}^*$  at higher temperatures.

Nevertheless, the effect on mean  $d_{\text{eff}}$  as a result of enhanced  $N_c$  at cold temperatures is inferred from two independent methods. In this study,  $N_c$  is calculated with the crystal size distribution whereas *S&O* use the residual particle number density. The mechanism is still an open question, but there are really only two possibilities why  $\text{Ci}$  would present an enhanced  $N_c$ . Either the cloud formed in air affected by aircraft exhaust nucleates more crystals, or contrails embedded in cirrus seed the cloud with a large number of small crystals. Anyhow, the perturbation affects a significant fraction of the cloud (c.f. Table 1, column 13), and any resulting radiative forcing caused by a change in optical properties has to be added to the forcing from that due to additional cloudiness. Note that the data presented here represent diluted plumes away from the direct emission.

The distinction between  $\text{Ci}^*$  and  $\text{Ci}$  was based on the amount of absorbing material present in the crystals. With a more sensitive instrument at hands, more data points would perhaps be classified as  $\text{Ci}^*$ . Since the study was performed over continental Europe, it is possible that the comparison between  $\text{Ci}^*$  and  $\text{Ci}$  actually reflect a varying degree of pollution. Comparing properties with cirrus formed in truly pristine conditions might give a different result, but it would in practice require making observations in the Southern Hemisphere midlatitudes.

**Acknowledgments.** This work is in part supported by the European Union through the AEROCONTRAIL project and by the Swedish Natural Science Council, NFR.

## References

- Boucher, O., Air traffic may increase cirrus cloudiness, *Nature*, **397**, 30-31, 1999.
- Darlison, A. G. and P.R. Brown, The use of automatic particle recognition to improve the determination of bulk quantities from PMS 2-D Probe Data in Cirrus, Proceeding 10th Int. Cloud Physics Conf. Bad Homburg FRG, August 15-20, 1988, 138-140.
- Dowling, D. R., and L. F. Radke, A Summary of the Physical Properties of Cirrus Clouds, *J. Appl. Meteor.*, **29**, 970-978.
- Dye, J. E. and D. Baumgardner, Evaluation of the forward scattering spectrometer probe. Part I: Electronic and optical studies, *J. Atmos. Oceanic Technol.*, **1**, 329-344, 1984.
- Fahey, D. W., and U. Schumann, Aviation-produced aerosols and cloudiness, Chapter 3 of IPPC, 1999 (to appear).
- Gayet, J.-F., G. Febvre and H. Larsen, The Reliability of the PMS FSSP in the Presence of Small Ice Crystals, *J. Atmos. Oceanic Technol.*, **13**, 1300-1301, 1996a.
- Gayet, J.-F., G. Febvre, G. Brogniez, H. Chepfer, W. Renger and P. Wendling, Microphysical and Optical Properties of Cirrus and Contrails: Cloud Field Study on 13 October 1989, *J. Atmos. Sci.*, **53**, 126-138, 1996b.
- Jensen, E. J. and O. B. Toon, The potential impact of soot particles from aircraft exhaust on cirrus clouds, *Geophys. Res. Lett.*, **24**, 249-252, 1997.
- Knollenberg, R. G., The optical Array: An Alternative to Scattering or Extinction for Airborne Particle Size Determination, *J. Appl. Meteor.*, **9**, 86-103, 1969.
- Kärcher, B., R. Busen, A. Petzold, F.P. Schröder, U. Schumann, and E.J. Jensen, Physicochemistry of aircraft-generated liquid aerosols, soot, and ice particles. 2, Comparison with observations and sensitivity studies, *J. Geophys. Res.*, **103**, 17111-17128, 1998.
- Larsen, H., J.-F. Gayet, G. Febvre, H. Chepfer and G. Brogniez, Measurement errors in cirrus cloud microphysical properties, *Ann. Geophys.*, **16**, 266-276, 1998.
- Mannstein, H., R. Meyer, and P. Wendling, Operational detection of contrails from NOAA-AVHRR-data, *Int. J. Remote Sensing*, 1999 (in press).
- Meerkötter, R., U. Schumann, D.R. Doelling, P. Minnis, T. Nakajima, and Y. Tushima, Radiative forcing by contrails, *Ann. Geophys.*, **17**, 1080-1094, 1999.
- Noone, K. J., J. A. Ogren, J. Heintzenberg, R. J. Charlson and D. S. Covert, Design and Calibration of a Counterflow Virtual Impactor for Sampling of Atmospheric Fog and Cloud Droplets, *Aerosol Sci. Technol.*, **8**, 235-244, 1988.
- Rogers, R. R. and M. K. Yau, *A Short Course in Cloud Physics*, Pergamon Press, Exeter, Great Britain, 1989.
- Schumann, U., J. Ström, R. Busen, R. Baumann, K. Gierens, M. Krautstrunk, F.P. Schröder, and J. Stingl, In situ observations of particles in jet aircraft exhausts and contrails for different sulfur containing fuels, *J. Geophys. Res.* **101**, 6853-6869, 1996.
- Schröder, F. and J. Ström, Aircraft measurements of sub micrometer aerosol particles ( $> 7 \text{ nm}$ ) in the midlatitude free troposphere and tropopause region, *Atmos. Res.*, **44**, 333-356, 1996.
- Ström, J., B. Strauss, F. Schröder, T. Anderson, J. Heintzenberg, P. Wendling, In-situ observations of microphysical properties of young cirrus clouds, *J. Atmos. Sci.*, **54**, 2542-2553, 1997.
- Ström, J. and S. Ohlsson, In-situ measurements of enhanced crystal number densities in cirrus clouds caused by aircraft exhaust, *J. Geophys. Res.*, **103**, 11355-11361, 1998.
- Wyser, K. and J. Ström, A possible change in cloud radiative forcing due to aircraft exhaust, *Geophys. Res. Lett.*, **25**, 1673-1676, 1998.

A. Kristensson, ITML, Stockholm University, S-106 91 Stockholm, Sweden. (e-mail: adam@itm.su.se)

(Received July 19, 1999; revised October 20, 1999; accepted January 7, 2000.)